Journal of the European Ceramic Society **9** (1992) 407–415

Corrosion of Technical Ceramics by Molten Aluminium

U. Schwabe, L. R. Wolff, F. J. J. van Loo & G. Ziegler*

Eindhoven University of Technology Centre for Technical Ceramics (CTK), P.O. Box 513, 5600 MB Eindhoven, The Netherlands

(Received 19 July 1990; revised version received 27 August 1991; accepted 29 August 1991)

Abstract

Corrosion investigations with various types of nonoxide technical ceramics, eight silicon nitride materials (1 grade of HIPRBSN, 3 grades of HPSN and 4 grades of RBSN), and two types of silicon carbide (HIPSiC and SiSiC) were carried out in aluminium melts (pure aluminium and AlZnMgCu1·5). HIPRBSN and HPSN materials exhibit nearly no corrosion attack under the most severe conditions applied (1000°C for 750 h). RBSN materials with relatively high open porosity are attacked after relatively short times. HIPSiC is considerably more attacked than HIPRBSN and the HPSN materials; however, it is also fairly corrosion resistant. SiSiC reveals the poorest corrosion behaviour of the materials investigated. The results are explained in terms of thermodynamics, diffusion through the metal/ceramic interface and wetting effects.

Es wurden an verschiedenen technisch bedeutsamen nichtoxidischen Keramiken Korrosionsversuche in Aluminiumschmelzen (reines Aluminium und AlZnMgCu1·5) durchgeführt. Getestet wurden acht Si_3N_4-Materialien (1 HIPRBSN, 3 HPSN und 4 RBSN) und zwei SiC-Materialien (HIPSiC und SiSiC). Die HIPRBSN- und HPSN-Werkstoffe zeigten selbst unter den härtesten Bedingungen (1000°C, 750 h) nahezu keine Korrosionserscheinungen. Das RBSN-Material mit einer relativ hohen offenen Porosität wurde dagegen schon nach relativ kurzer Zeit angegriffen. Das HIPSiC wird zwar wesentlich stärker angegriffen als das HIPRBSN und HPSN, jedoch ist es ebenfalls relativ korrosionsbeständig. Der SiSiC-Werkstoff zeigte die schlechteste Korrosionsbeständigkeit aller getesteten Materialien. Die Ergebnisse werden anhand thermodynamischer Betrachtungen, der Diffusion durch die Metall/Keramik-Grenzfläche und des Benutzungsverhaltens diskutiert.

On a conduit des études de corrosion dans des fondus d'aluminium (aluminium pur et AlZnMgCu1·5) sur différentes céramiques techniques non-oxyde: 8 types de nitrure de silicium (1 HIPRBSN, 3 HPSN, 4 RBSN) et 2 types de carbure de silicium (HIPSiC et SiSiC). Les matériaux HIPRBSN et HPSN ne présentaient quasiment pas d'attaque de corrosion dans les conditions les plus sévères (1000°C, 750 h). Les matériaux RBSN à porosité ouverte relativement élevée étaient facilement attaqués après un temps relativement court. Le HIPSiC, bien que présentant une bonne résistance à la corrosion, était considérablement plus attaqué que le HIPRBSN et que les HPSN. Le matérial SiSiC présentait le comportement en corrosion le plus faible de la série. On interprète ces résultats en termes de themodynamique, de diffusion à l'interface métal/céramique et d'effets de mouillage.

1 Introduction

For metallurgical applications of technical ceramics like silicon nitride, silicon carbide, aluminium oxide, zirconium oxide, aluminium titanate and boron nitride, it is important to have knowledge of the corrosion behaviour of these materials in metal melts. Knowledge of the joining of metals with ceramics, including metal/ceramic composites and cermets is also of great value, because in the joining of ceramics to metals similar physical and chemical effects occur. Recently, silicon nitride bonded silicon

* Present address: University of Bayreuth, Institute of Materials Research (IMA), P.O. Box 101251, 8580 Bayreuth, FRG.

Journal of the European Ceramic Society 0955-2219/92/$5.00

carbide ceramic materials have gained special interest in the form of immersion tubes for indirect heating of aluminium melts.[1]

In this study corrosion tests in aluminium melts were carried out on various silicon nitride and silicon carbide materials using different testing methods. Thermodynamic considerations were made on corrosion reactions. Experimental results and theoretical considerations including thermodynamics, diffusion through the metal/ceramic interface and wetting effects are used together to come to a better understanding of the corrosion behaviour of these ceramic materials.

2 Thermodynamics

Of particular importance for planning tests as well as for interpreting the test results are thermodynamic considerations on corrosion reactions. With thermochemical data[2,3] and binary phase diagrams[4,5] known from the literature ternary phase diagrams for the systems Al–Si–N and Al–Si–C were constructed for 827°C and 1027°C, only considering the main products which might be formed. These diagrams are shown in Fig. 1.

The following reactions have to be considered with Si_3N_4 and Al in the temperature range between 827°C and 1027°C:

$$Si_3N_4 + 4Al = 4AlN + 3Si \quad (1)$$

$$Si_3N_4 = 2N_2\uparrow + 3Si \quad (2)$$

$$Si + xAl = \{Si\text{–}Al_x\} \quad (3)$$

Si_3N_4 reacts with Al in the temperature range between 827 and 1027°C and solid Si and AlN are formed (reaction (1)). Moreover, Si_3N_4 may dissociate into N_2 and solid Si (reaction (2)). The solid

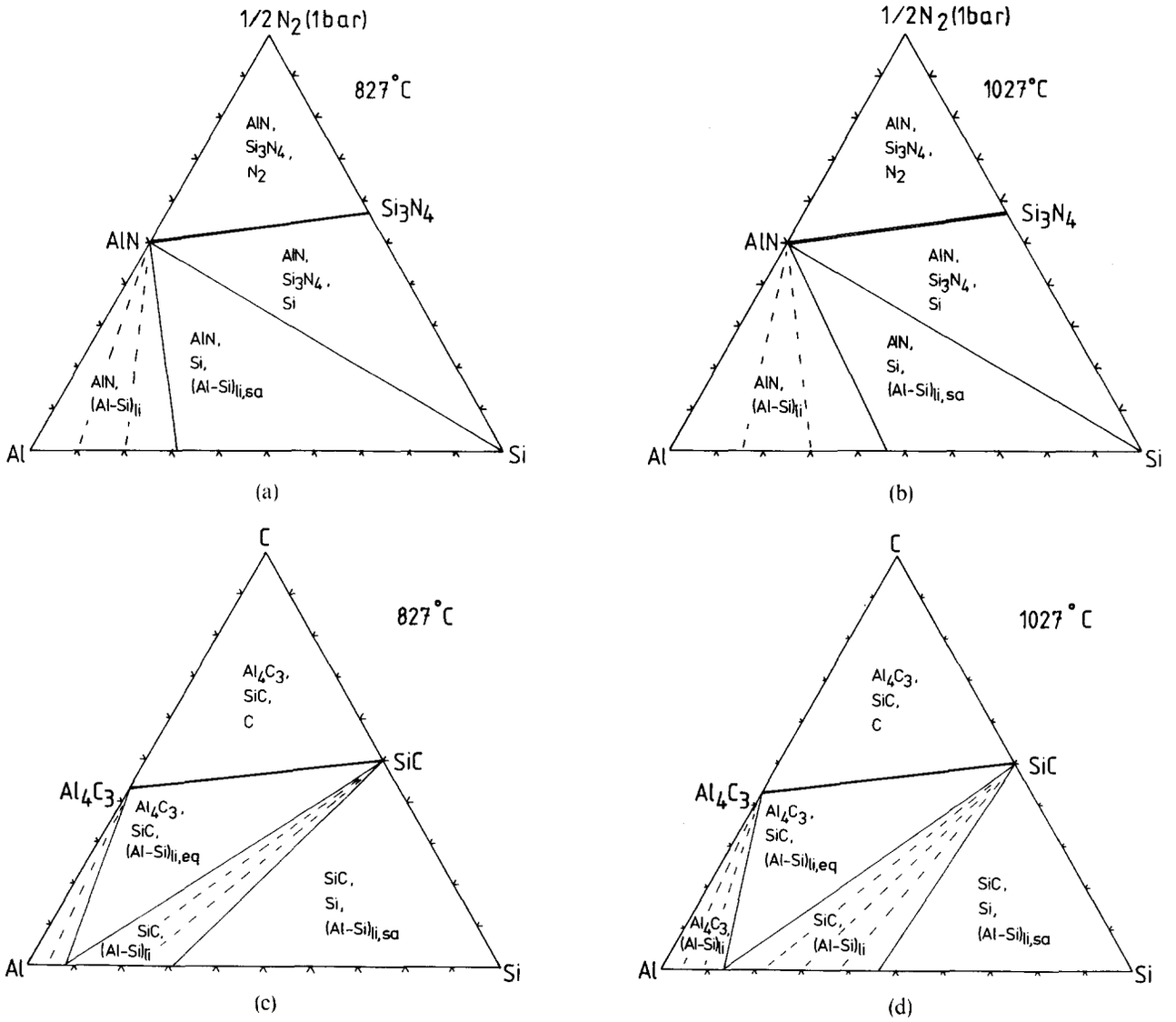

Fig. 1. Ternary phase diagrams for the systems Al–Si–N ((a) and (b)) and Al–Si–C ((c) and (d)) at 827°C ((a) and (c)) and 1027°C ((b) and (d)).

silicon formed can dissolve in the liquid aluminium (reaction (3)).

Reaction (1) is thermodynamically strongly favoured in the temperature range discussed. Reaction (2) can proceed in a gas atmosphere with a N_2 pressure low enough, for 827°C lower than 10^{-4} Pa and for 1027°C lower than 5×10^{-2} Pa, calculated from thermochemical data given in Ref. 2. Reaction (1) and reaction (2) are coupled with reaction (3). If, at a given temperature, saturation of the Al–Si melt is reached, solid Si will be formed. The dissolution of Si in the melt lowers the activity of Si, and thus enhances the decomposition reaction (1).

For SiC and Al only two reactions have to be considered:

$$3SiC + 4Al = Al_4C_3 + 3Si \qquad (4)$$

and reaction (3).

For reaction (4) the equilibrium lies on the left hand side. However, in combination with reaction (3) an equilibrium exists between SiC, Al_4C_3 and a liquid mixture. In contrast to the Al–Si–N system the reaction product (Al_4C_3) can not coexist with pure solid Si. The calculated equilibrium composition of the liquid Al–Si mixture in this system is largely dependent on small changes in Gibbs enthalpies, so that the variations in the values found in the literature can easily be explained by these changes. Viala *et al.*[3] determined experimentally the equilibrium silicon concentrations as a function of temperature. Heikinheimo *et al.*[6] calculated the equilibrium Si concentration at 1000°C, and Warren & Andersson[7] estimated a plausible equilibrium value at 800°C. All these values are compiled in Table 1.

The temperature dependence of the Gibbs enthalpies of some important corrosion reactions of nitrides, carbides and oxides with molten aluminium is given in Fig. 2. For the silicon nitride materials the following reactions may influence the corrosion behaviour: the thermodynamically strongly favoured reaction of aluminium with the main component silicon nitride and the reactions with the

Table 1. Temperature dependence of silicon content in the liquid Al–Si phase in equilibrium with SiC and Al_4C_3

Temperature (°C)	*Si (atom %)*		
	Reference 3	*Reference 6*	*Reference 7*
750	5·6		
800	7·4		7
827	8·2		
1 000	12·9	16	
1 027	13·4		
1 300	16·1		

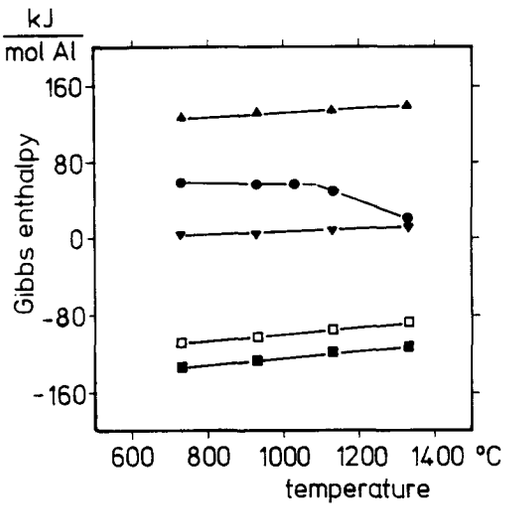

Fig. 2. Temperature dependence of Gibbs enthalpies of some important corrosion reactions considering Si_3N_4, SiC and some oxides which are essential for the materials investigated.

□ $Si_3N_4 + 4Al = 4AlN + 3Si$
▲ $Y_2O_3 + 2Al = Al_2O_3 + 2Y$
● $3MgO + 2Al = Al_2O_3 + 3Mg$
▼ $3SiC + 4Al = Al_4C_3 + 3Si$
■ $3SiO_2 + 4Al = 2Al_2O_3 + 3Si$

sintering additives yttria and magnesia. It is clear that the formation of liquid alloys of Al with Si, Y and Mg will promote the corrosion reaction. The sintering additive yttria is very stable in contact with molten aluminium, and thus less susceptible to corrosion attack. The thermodynamical stability of the sintering additive magnesia in liquid aluminium is not so high, but the equilibrium is still on the left hand side. However, the reaction becomes possible if the volatile reaction product Mg is removed by evaporation from the melt, especially at high temperatures. For the corrosion of silicon carbide materials the reaction of SiC with Al is near the thermodynamical equilibrium, so that the driving force is much less than for Si_3N_4. For both groups of materials, silicon nitride and silicon carbide, the reaction of silica, present in the oxide layers on the ceramic surface, with the aluminium melt is thermodynamically strongly favoured.

3 Experimental Procedure

3.1 Corrosion tests

Three types of tests were used, two short-term tests and one long-term test. The short-term tests were performed as follows:

—Graphite crucibles (inner diameter 10 mm, inner height 20 mm) were provided with small nearly cubic ceramic samples (5 × 5 × 5 mm) together with 2·5 g pure aluminium (Al 99·99%)

and heated in tube furnaces in flowing helium. In some experiments the graphite crucibles were replaced by high-purity alumina crucibles, and additionally an alumina boat with coal granules was placed upstream in the hot zone near by the crucibles.

—Crucibles of the ceramic materials to be tested (inner diameter 21 mm, inner height 25 mm) were provided with 2·5 g of a commercial aluminium alloy (AlZnMgCu1·5—composition (in wt%): Zn, 5·6–6·1; Mg, 2·1–2·9; Cu, 1·2–2·0) and heated in a tube furnace with flowing helium atmosphere.

In the first type of short-term test the test temperature was kept at 1000°C over 48 h with the exception of the varied method, where test time was 96 h, and additionally a test temperature of 750°C was applied. In the second type of short-term test the temperature of 1000°C was kept for 48 h. The oxygen content of the gas leaving the furnace was monitored with a ZrO_2–oxygen sensor, the oxygen partial pressure was 10^{-15} Pa.

In the long-term tests ceramic samples with the same dimensions as in the first type of short-term test were placed together with 10 g pure aluminium (Al 99·99%) in crucibles made of inert material (stabilized zirconium oxide: inner diameter 22 mm, inner height 28 mm) covered with a graphite plate and placed in a graphite crucible holder. The test temperature of 1000°C was kept over 500 and 750 h respectively.

3.2 Materials

Eight silicon nitride materials and two types of silicon carbide were investigated:

- Hot-isostatically pressed reaction-bonded silicon nitride (HIPRBSN) with 4·2 wt% Y_2O_3 as sintering additive: density 100% th.d., β-Si_3N_4, crystalline Y–Si–O–N secondary phases, partly amorphous grain boundary phases.
- Hot-pressed silicon nitride (HPSN) with 11 wt% Y_2O_3 as sintering additive: density 100% th.d., β-Si_3N_4, crystalline Y–Si–O–N secondary phases, partly amorphous grain boundary phase.
- Hot-pressed silicon nitride (HPSN) with 2·5 wt% MgO as sintering additive: density 100% th.d., β-Si_3N_4, crystalline Mg–Si–O–N secondary phases, mostly amorphous grain boundary phase.
- Hot-pressed silicon nitride (HPSN) with 5 wt% MgO as sintering additive: density 100% th.d., β-Si_3N_4, crystalline Mg–Si–O–N secondary phase, mostly amorphous grain boundary phase.
- Reaction-bonded silicon nitride (RBSN): 18·6% open porosity, average micropore size 0·10 μm, phase composition of Si_3N_4 $\alpha/(\alpha+\beta) = 0{\cdot}92$, about 3 wt% free silicon.
- Reaction-bonded silicon nitride (RBSN): 21·6% open porosity, average microphore size 0·07 μm, phase composition of Si_3N_4 $\alpha/(\alpha+\beta) \cong 0{\cdot}8$.
- High-purity reaction-bonded silicon nitride (RBSN): 23·2% open porosity, average micropore size 0·07 μm, phase composition of Si_3N_4 $\alpha/(\alpha+\beta) \cong 0{\cdot}8$, less than 0·1 wt% free silicon.
- Reaction-bonded silicon nitride (RBSN): 22·9% open porosity, average micropore size 0·19 μm.
- Hot-isostatically pressed silicon carbide (HIPSiC) with 0·2 wt% Al: density 100% th.d.
- Infiltrated silicon carbide (SiSiC): free silicon content about 12 wt%.

3.3 Characterization methods

Microstructural changes after corrosion attack were investigated by light microscopy, scanning electron microscopy (SEM) including energy dispersive analysis (EDX), electron probe microanalysis and X-Ray diffraction analysis.

4 Results

4.1 Silicon nitride

4.1.1 Hot-isostatically pressed reaction-bonded silicon nitride with 4·2 wt% Y_2O_3

This material was submitted to long-term testing. X-Ray mapping and line scans of aluminium, silicon, yttrium, nitrogen and oxygen shows that during the long-term tests over 500 and 750 h respectively a dense reaction layer of an average thickness of about 6 μm was formed. Besides AlN, as expected from thermodynamics, oxygen was also found in this layer. In the metal near the metal/ceramic interface aluminium oxide particles were observed.

The oxygen and the Al_2O_3 particles obviously derive from the oxide layer always surrounding the aluminium and, regarding the oxygen, to a minor extent from the oxide layer on the silicon nitride. Which role the sintering additive yttria plays in the formation of the interface is still not clear. From the composition of the reaction layer (Al, Y, Si, O, N) it might be assumed that a (Y)SiAlON layer is formed. The wetting of Si_3N_4 by the aluminium melt is poor.

4.1.2 Hot-pressed silicon nitride with 11 wt% Y_2O_3

After long-term testing X-ray mappings and line

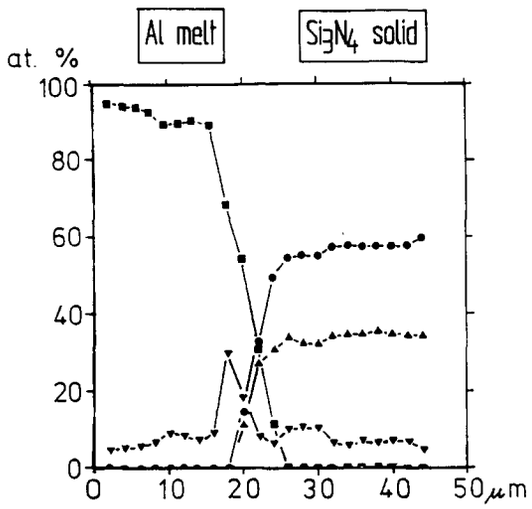

Fig. 3. Line scan of the interlayer between Al and Si_3N_4 after 750 h at 1000°C for hot-pressed Si_3N_4 with 11 wt% Y_2O_3. ■, Al; ●, Si; ▲, N; ▼, O.

scans show similar results as with HIPRBSN. In the line scan, presented in Fig. 3, the thickness of the interlayer between metal and ceramic (5 μm) is minimally smaller than in HIPRBSN. The wetting is also poor.

4.1.3 Hot-pressed silicon nitride with 2·5 wt% MgO

After long-term testing the roughness of the interface between the metal and the ceramic is higher than for the two ceramic materials already discussed. This may be an indication that a stronger (or another) form of corrosion attack has occurred than in the case of Y_2O_3-doped materials. The following reasons may account for this: Firstly, the sintering additive MgO behaves in a different way to Y_2O_3 in contributing to the formation of a corrosion-inhibiting interlayer between the metal and the ceramic. Secondly, the X-ray mapping for Mg and the concentration profiles for Mg across the interface determined by line scans show a strong variation in Mg concentration over the specimen, which may result from the different corrosion attack at various places. As in the two Y_2O_3-doped materials already described, the X-ray mappings and the line scans for the elements Al, Si, Mg, O, N show a thickness of around 6 μm, where all elements are found together. The composition of this layer might be an indication of the formation of a (Mg)SiAlON layer. Also with this material the wetting is found to be poor.

4.1.4 Hot-pressed silicon nitride with 5 wt% MgO

The effect of the sintering additive MgO on the corrosion attack observed after long-term testing is seen more clearly than with 2·5 wt% MgO. In Fig. 4

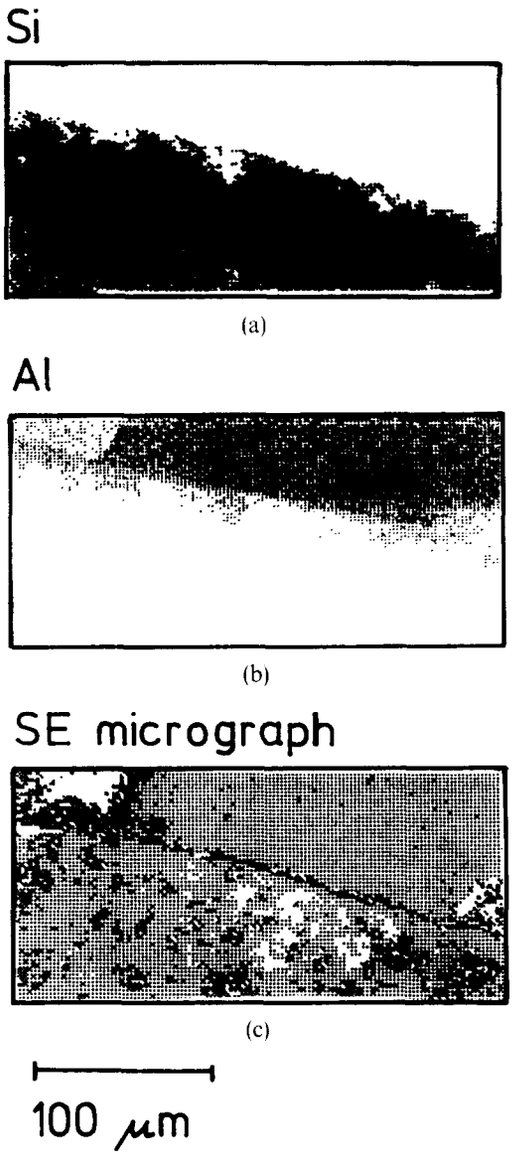

Fig. 4. X-Ray maps for (a) Si, (b) Al and (c) secondary electron micrograph of the metal/ceramic interface of Si_3N_4 (5 wt% MgO)/Al 99·99 after 312 h at 1000°C (metal is on top).

the X-ray mappings for Al and Si and the secondary electron micrograph show the local attack of the ceramic without any change in the surface morphology.

4.1.5 Reaction-bonded silicon nitride with 18·6% open porosity

After the first short-term test SEM investigations showed strong changes in microstructure of the ceramic material. As expected, porosity has decreased considerably. X-Ray diffraction analysis of the ceramic material proves the formation of about 80% aluminium nitride, as expected from thermodynamics. Consequently, the silicon nitride content had decreased and some aluminium metal was found. In the aluminium metal a few per cent of silicon was detected with SEM/EDX.

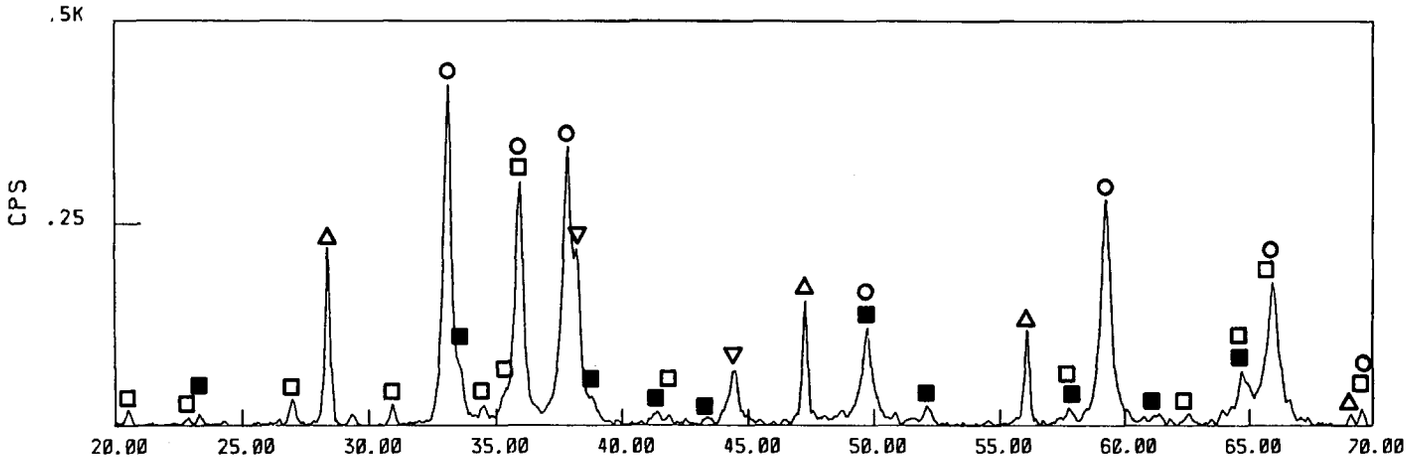

Fig. 5. X-Ray diffraction analysis of the infiltrated part of the RBSN crucible after the corrosion test in aluminium alloy melt (AlZnMgCu1·5) at 1000°C. □, α-Si_3N_4; ■, β-Si_3N_4; ○, AlN; △, Si; ▽, Au. (The sample was coated before with gold for SEM investigation.)

4.1.6 Reaction-bonded silicon nitride with 21·6% open porosity

With this material the second short-term test was carried out. Infiltration throughout the thickness of the bottom (3·5 mm) takes place, indicated by SEM/EDX examination and by X-ray maps for the elements aluminium and silicon. X-Ray diffraction analysis of the infiltrated ceramic part results in the following phases: a large amount of AlN and some Si, as well as a small amount of α- and β-Si_3N_4 (Fig. 5). The macroscopic wetting angle varied between 60° and 110°.

4.1.7 High-purity reaction-bonded silicon nitride with 23·2% open porosity

With this material the varied first short-term test was carried out at 750°C and 1000°C. At 750°C no wetting and no reaction was found. On the other hand, at 1000°C as with other open porous RBSN materials, the ceramic was completely penetrated with melt and nearly completely converted to AlN. Compared to commercially available RBSN with 22·9% open porosity, no significant difference in the corrosion attack could be observed.

4.2 Silicon carbide

4.2.1 Hot-isostatically pressed silicon carbide with 0·2 wt% Al

This material was submitted to the long-term tests. Because the possible reaction product aluminium carbide is known to be very susceptible to hydrolysis by liquid water and even humidity of the atmosphere, a special method was used for preparing the samples for SEM/microprobe measurements, excluding water. A reaction layer of roughly 100 μm thickness was found. Microprobe measurements showed that the layer consists of grains of aluminium carbide of about 4–5 μm diameter, the space in between these grains of 1–2 μm is filled with Al–Si alloy. This can be seen by Al and Si X-ray analysis. A concentration profile over the layer thickness does not exist.

4.2.2 Infiltrated silicon carbide (SiSiC) with 12 wt% free silicon

After the short-term test 1 SEM investigations showed a strong change in microstructure of the SiSiC material. A corrosion layer of about 500–600 μm consisting of Al_4C_3 was found. Inside the ceramic material the grains of silicon carbide were partially corroded, as indicated by changes in grain shape. The silicon between the silicon carbide grains was partially replaced by aluminium. The silicon content of the melt was found to be only a few per cent.

5 Discussion

5.1 Silicon nitride

As expected, a fundamental difference is observed between the behaviour of dense and open porous silicon nitride. Dense silicon nitride shows nearly no corrosion attack even after long-term testing at 1000°C over 750 h, whereas porous silicon nitride has already extensively reacted after 48 h under the same conditions. Various reasons for this different behaviour might be responsible:

- Due to the high open porosity the interface which can react with the melt is much larger in RBSN than in dense materials.
- The irregular curved pore surface of the porous

materials complicates the formation of a closed corrosion inhibiting interface layer. Reaction layers have been found by various investigators.[8–14]

- Reaction-bonded silicon nitride may contain small amounts of free silicon from the production process, which easily dissolves in liquid aluminium (reaction (3)), and thus, may have two effects to promote wetting and reaction.[15] Free silicon enhances wetting of the ceramic and the dissolution of the silicon in liquid aluminium increases the contact interface. As a consequence, the reaction rate between ceramic material and metal is enhanced.
- The silica layer on the greater inner surface of the open pores may have an additional effect in improving wetting due to the reduction to silicon by aluminium.
- Reaction-bonded silicon nitride (which is not subjected to sintering after reaction bonding) contains no sintering additives, so that reaction products are not so effective in inhibiting corrosion attack.
- Another possibility, already discussed in a previous paper,[16] is the additional occurrence of the decomposition reaction of silicon nitride (reaction (2)), which is, for example, the only possible corrosion reaction of Si_3N_4 with copper.[17]

Which of these factors are decisive and of practical importance has to be investigated in further tests with RBSN materials where the parameters open porosity, pore shape, silicon content are systematically varied. The influence of surface modifications by very pure silicon nitride layers (applied e.g. by CVD) should also be included in these considerations.

In all materials AlN is formed. This is in agreement with thermodynamics. However, in dense silicon nitride the secondary phase composition has to be considered. The differences in corrosion behaviour between the various types of dense silicon nitride are found to be not so essential. However, there are some indications that small variations between the Y_2O_3-fluxed and MgO-doped materials exist. The greatest distinction is to be seen in a local attack in the MgO containing materials. However, it is not yet clear whether these differences are due to the different type of additives or due to concentration inhomogeneities. In Ref. 17 it was found that MgO-fluxed silicon nitride was attacked more strongly by Cu than materials containing Al_2O_3 or β'-SiAlONs. In both materials oxygen was found in the reaction layer, so that a formation of SiAlON(s) might be considered. Perhaps MgO and Y_2O_3 may be in some way involved in the formation of this layer. These thin layers, found in all dense silicon nitride materials investigated till now, account for the corrosion resistance of these materials.

5.2 Silicon carbide

As expected, with silicon carbide materials a strong distinction in corrosion behaviour has to be made between dense silicon carbide and silicon infiltrated silicon carbide. Dense silicon carbide forms a layer remarkably thicker than that on dense silicon nitride. Because of the greater thickness the microstructure of this layer can be investigated in more detail. The reaction product is Al_4C_3, which is the only product of the corrosion reaction of SiC with Al after reaction (4) in the temperature range between 650°C and about 1350°C (see Section 2 and Ref. 3). The microstructure of the layer explains the larger corrosion effect compared to dense silicon nitride. At the test temperature the interspaces between Al_4C_3 grains are filled with liquid Al–Si alloy. This liquid alloy allows a much faster exchange of material through the interface than solid-state diffusion in the case of silicon nitride.

Silicon-infiltrated silicon carbide is attacked very easily by dissolving the free silicon between the silicon carbide grains. The now isolated silicon carbide grains exhibit an extensive interface to the melt, and thus are strongly attacked. As in the case of RBSN, the free silicon increases the wetting behaviour.

The results of the investigations with dense silicon nitride and silicon carbide after long-term testing are summarized in Fig. 6.

Comparison with results on oxidized SiC–Si_3N_4

Recently a paper was published by Johnston & Little[1] concerning the degradation of oxidized silicon nitride bonded silicon carbide in molten

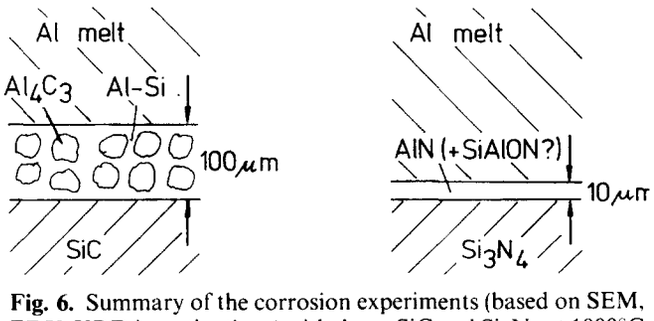

Fig. 6. Summary of the corrosion experiments (based on SEM, EDX, XRD investigations) with dense SiC and Si_3N_4 at 1000°C for 750 h (schematic).

aluminium. The results are compared with those described here.

The ceramic material used in Ref. 1 was a composite consisting of dense SiC grains reaction bonded with open porous silicon nitride with 17% porosity and some oxynitride content. Samples of this material were subjected to an immersion corrosion test at 750°C for 168 h in an Al–Si alloy with 12 wt % silicon before and after oxidation in air at 1000°C for 48 and 138 h respectively.

The nonoxidized samples showed no significant corrosion attack, whereas oxidized samples are readily attacked on the silicon nitride phase. According to the authors this behaviour is caused by the formation of a silica layer preferably on the large surface of the porous silicon nitride. This silica layer is readily wetted and attacked by the aluminium melt under formation of silicon and alumina. Subsequently the oxidized silicon nitride can be attacked by the liquid aluminium. Silicon carbide cannot react with Al under these conditions for thermodynamic reasons: The silicon content of the metal melt is, at 12 wt % Si ($\cong$ 12 at.% Si), higher than the equilibrium concentration at this temperature of about 5·6 at.% in contact with SiC and Al_4C_3.

The findings with the nonoxidized material are in accordance with the results of this investigation: open porous reaction-bonded silicon nitride materials did not react with aluminium at temperatures lower than 800°C, although strongly favoured by thermodynamics. Dense silicon carbide, although it is allowed by thermodynamics to react with pure aluminium to a great extent, only forms a thin layer of reaction products of about 100 μm thickness even at 1000°C for 750 h, far from reaching equilibrium.

6 Conclusions

Reaction products observed in the various materials investigated are in good agreement with thermodynamic predictions. However, depending on the microstructure of the materials controlled by different processing techniques, the interaction between silicon nitride or silicon carbide and the aluminium melt is quite different.

On dense silicon nitride a thin and dense corrosion inhibiting layer of mainly AlN is formed. This mechanism does not work with open porous RBSN, which reacts extensively with the aluminium melt at 1000°C, while at 750°C no wetting or reaction is observed. The temperature limit for the formation of the reaction products is about 800°C. The influence of sintering additives is up to now not clear and is the subject of further investigations.

With dense silicon carbide an interlayer is formed consisting of Al_4C_3 grains with interspaces filled with liquid Al–Si alloy, which does not act as effectively as a corrosion barrier as the layer on dense silicon nitride does. Silicon-infiltrated silicon carbide is very prone to corrosion attack, because of its free silicon content.

For both reaction-bonded silicon nitride and silicon-infiltrated silicon carbide, free silicon is assumed to enhance wetting, and in consequence, corrosion attack.

Comparison of the experiments with open porous reaction-bonded silicon nitride and dense silicon carbide in this work with the results obtained in Ref. 1 with a composite material consisting of dense SiC grains reaction bonded by silicon nitride allows the following additional conclusions. A silica layer formed by oxidation of the porous reaction-bonded silicon nitride increases wetting and the reaction rate in contact with aluminium melt so that detrimental corrosion can already occur at 750°C in the silicon nitride. Oxidation of silicon nitride ceramics has to be avoided, because the formation of silica is particularly disadvantageous by increasing wetting.

As a consequence, the following conceptions can be established to improve corrosion resistance of technical ceramic materials. With materials thermodynamically not stable towards the metal melt the corrosion resistance of a material can be improved by making or keeping the surface non-wetting. This is especially of importance with open porous materials, where infiltration of the melt into the pores has to be avoided. Possibilities to achieve this aim are to reduce the wettability by surface layers and/or to close the pores by e.g. PVD or CVD layers.

Acknowledgement

The authors gratefully acknowledge the sponsorship of the work by the IOP Programme Commission of the Government of the Kingdom of The Netherlands.

References

1. Johnston, M. W. & Little, J. A., Degradation of oxidized SiC–Si_3N_4 in molten aluminium. *J. Mater. Sci.*, **25** (1990) 5284–90.
2. Barin, I., Knacke, O. & Kubaschewski, O., *Thermochemical Properties of Inorganic Substances*, 1973 and Supplement 1977. Springer-Verlag, Berlin/Heidelberg.
3. Viala, J. C., Fortier, P. & Bouix, J., Stable and metastable phase equilibria in the chemical interaction between

aluminium and silicon carbide. *J. Mater. Sci.*, **25** (1990) 1842–50.
4. Hultgren, R., Desai, P. D., Hawkins, D. T., Gleiser, M. & Kelley, K. K., *Selected Values of the Thermodynamic Properties of Binary Alloys*. American Society for Metals, Metals Park, Ohio, 1973, pp. 210–12.
5. Schuster, J. C., Weitzer, E., Bauer, J. & Nowotny, H., Joining of silicon nitride ceramics to metals: The phase diagram base. *Materials Science and Engineering A*, **105/106** (1988) 201–6.
6. Heikinheimo, E., Savolainen, P. & Kivilahti, J., Phase equilibria in the silicon carbide–aluminium system. In *Proc. Conf. User Aspects of Phase Diagrams*, 25–27 June 1990, Petten, The Netherlands. The Institute of Metals, London, (in press).
7. Warren, R. & Andersson, C.-H., Silicon carbide fibres and their potential for use in composite materials. Part II. *Composites*, **15** (1984) 101–11.
8. Loehman, R. E., Interfacial reactions in ceramic–metal systems. *Am. Ceram. Soc. Bull.*, **68**(4) (1989) 891–6.
9. Loehman, R. E., Tomsia, A. P., Pask, J. A. & Johnson, S. M., Bonding mechanisms in silicon nitride brazing. *J. Am. Ceram. Soc.*, **73**(3) (1990) 552–8.
0. Brener, R., Edelman, F. & Gutmanas, E. Y., Formation of an interfacial AlN layer in an Al/Si_3N_4 thin-film system. *Appl. Phys. Lett.*, **54**(10) (1989) 901–3.
11. Ning, X. S., Suganuma, K., Okamoto, T., Koreeda, A. & Miyamoto, Y., Interfacial strength and chemistry of additive-free silicon nitride ceramics brazed with aluminium. *J. Mater. Sci.*, **24** (1989) 2879–83.
12. Ning, X. S., Okamoto, T., Miyamoto, Y., Koreeda, A. & Suganuma, K., Effect of oxide additive in silicon nitride on interfacial structure and strength of silicon nitride joints brazed with aluminium. *J. Mater. Sci.*, **24** (1989) 2865–70.
13. Suganuma, K., Okamoto, T., Koizumi, M. & Shimada, M., Joining of silicon nitride to silicon nitride and to Invar alloy using an aluminium interlayer. *J. Mater. Sci.*, **22** (1987) 1359–64.
14. Naka, M., Mori, H., Kubo, M., Okamoto, I. & Fujita, H., Observations of Al/Si_3N_4 interface. *J. Mater. Sci. Lett.*, **5** (1986) 696–8.
15. Milner, D. R., A survey of the scientific principles related to wetting and spreading. *Brit. Welding J.*, (1958) 90–105.
16. Schwabe, U., Wolff, L. R., van Loo, F. J. J. & Ziegler, G., Corrosion of technical ceramics by molten aluminium. In *Euro-Ceramics, Vol. 3, Engineering Ceramics*, ed. G. de With, R. A. Terpstra & R. Metselaar. Elsevier Science Publishers Ltd, London, 1989, pp. 3.522–3.526.
17. Sangiorgi, R., Bellosi, A., Muolo, M. L. & Babini, G. N., Corrosion of hot-pressed silicon nitride-based materials by molten copper. *J. Mater. Sci.*, **24** (1989) 4080–7.